HiSST: 3rd International Conference on High-Speed Vehicle Science Technology
14 -19 April 2024, Busan, Korea

Numerical Investigation of a Pulse Detonation Engine with Resonator Injection

T. Hemard[1]*, B. H. Saracoglu*[2]

Abstract

Pressure gain combustion technology has been heavily investigated by the research community due to its promising theoretical thermal efficiency superiority over constant pressure combustion systems. One of the major implementations of PGC is pulse detonation engines (PDE) whose aeronautical applicability has been proven at the beginning of the millennium. Present research highlighted in this paper aims at investigating the applicability of a PDE with Helmholtz resonator injection system for space thruster applications. In order to investigate the effect of Helmholtz resonator for PDE injection as a mixing enhancement device, a thorough numerical study has been performed using the commercial solver Ansys Fluent. Unsteady Reynolds-Averaged Navier-Stokes equations were solved over a fully featured computation domain of the pulse detonation thruster (PDT) using k-w SST turbulence closure and Arrhenius rates for detailed chemical reactions of H_2 and O_2. Unsteady wave motion on in the resonator and the mixer prior to the ignition has been recorded at thirteen probe locations and analyzed to understand the operation of the system to rapidly achieve detonable mixtures in short distances. The cold flow analysis showed that a detonable mixture can be achieved promptly while the hot flow simulations depicted a distinct combustion zone at the mixing region. A detailed analysis of the reactive flow within the PDT revealed a detailed overview of the operability of the PDT. The unsteady features within the flow field are investigated in detail both in time and frequency domain along with the propulsive performance of the PDT.

Keywords: Pulse Detonation Engines, Computation fluid dynamics, Satellite propulsion, Helmholtz resonator

Nomenclature

CFD	–	Computational fluid dynamics	URANS	–	Unsteady Reynolds-Averaged Navier-Stokes
CJ	–	Chapman-Jouget	P	-	Pressure
I	–	Impulse	PDE	–	Pulse detonation engine
M	–	Mach number	PDT	–	Pulse detonation thruster
SST	–	Shear Stress Transport	PGC	–	Pressure gain combustion
T	–	Temperature	ρ	–	Density
STFT	–	Short Time Fourier Transform			

[1] *Trainee, von Karman Institute for Fluid Dynamics, Waterloosesteenweg 72 B-1640 Sint-Genesius-Rode Belgium, timothee.hemard@vki.ac.be*
[2] *Research Expert, von Karman Institute for Fluid Dynamics, Waterloosesteenweg 72 B-1640 Sint-Genesius-Rode Belgium, bayindir.saracoglu@vki.ac.be*

1. Introduction

Detonation combustion process and engine architectures has been numerically and experimentally investigated by various research groups for several decades thanks to its higher theoretical thermal efficiency as compared to the systems based on deflagration combustion. Detonation is a very fast combustion process, converting significant amount of chemical energy to thermal energy. It has been estimated that a 20 m² detonation wave operates at the same power as is received by the Earth from the Sun [1]. Pulse Detonation Engines (PDEs) exploit detonative combustion to generate thrust inherently more than their current deflagrative counterparts owing to the simultaneous increase in both temperature and pressure [2]. Current aeroengines operating based on deflagrative combustion is thermodynamically characterized by the Brayton cycle (turbojets, ram/scramjets, etc.) while detonation-based engines are characterized by a variation of the Humphrey cycle. The main difference between the Humphrey cycle and the Brayton cycle is the change to a constant volume heat addition instead of a constant pressure one. Consequently, detonation engines does not require use of multi-stage compressors and other turbo-components, which augments the system weight and complexity systems, to pressurize the incoming air thanks to the pressure gain foreseen during the detonation process.

Multiple models have been visited to represent detonation process. One commonly used in literature is the Chapman-Jouguet (CJ) model [3]. Analytically speaking, the CJ point is obtained when the Rayleigh line and the Hugoniot curve, both derived from the Rankine-Hugoniot relations for ideal gases, have equal derivatives on p-v diagram. This forms a point, the CJ point, that distinguishes detonation from deflagration. These conditions, known as the CJ conditions, are used to characterize detonation properties and to provide an indicator for the analytical and numerical analysis of detonation. PDEs work on a cyclic process which follows distinct phases of operation in 4-steps: mixture injection, detonation initiation, detonation propagation and blow down where the combustion products are expelled to generate thrust. The fuel and oxidizer mixing can be achieved using mechanical valves or acoustic resonators to achieve proper mixture conditions to efficiently detonate the combustible stream. The valve based PDEs requires a dedicated control system to synchronize the injection of the reactants with ignition which resonator system can enhance mixing and promote better injection dynamics without using many moving parts [4]. Helmoltz resonators, also used for the current research, are simple acoustic devices that generate acoustic resonance at a given frequency depending on their geometric and material properties. Using resonators within the injection systems allows to generate turbulence and improve mixing efficiency with limited added complexity. Such systems have been investigated for many years to simplify the ignition of rocket engines. [5]

The common architecture of a pulse detonation engine contains a long tube (thrust tube) that includes 3 main sections: the thrust end where injection and ignition takes place, the detonation section where the reactants detonate, or gone through deflagration to detonation transition process, and the final blow down section where the products directly expand to the outside medium or expands through a nozzle . Such simplistic architecture of the PDE allows to achieve efficient thrust generation with fewer moving parts, lower weight, and relatively lower cost [3].

PDEs implementation for various applications are still under development. However, the applicability of the technology for aeronautical application was demonstrated through the flight of the Long E-Z aircraft powered by 4 PDEs from Mojave Air Field [6]. Similar works has been performed on a wide range of concepts, from multitube self-igniting PDE's to using resonating chambers to have a self-aspirating engine[4] [7]. Moreover, very large operational envelope of PDE also made them attractive to the other research groups for single stage to orbit (SSTO) vehicles and satellite propulsion, where the ambient medium affects the engine significantly less for PDEs than traditional engines [8].

The current study concentrates on the flow field analysis and performance estimations of a pulse detonation engines using a resonation injection system through unsteady numerical simulations under both inert and reactive flow conditions. The paper summarizes the numerical methodology used, and computational grid design with mesh convergence study, the analysis of the cold flow and reactive flow results.

2. Methodology

2.1. Numerical tool

Computational fluid dynamics solver Ansys Fluent was utilized to perform reactive and non-reactive Unsteady Reynold-Averaged Navier-Stokes (URANS) simulations using finite volume approach for all the computations included in this study. Continuity, momentum, energy and species continuity equations are solved in three-dimensions using AUSM flux scheme with 2nd order upwind method to calculate fluxes, turbulent kinetic energy and specific dissipation rate. Turbulence closure was achieved with k-ω SST (Shear Stress Transport) model. A compressible ideal gas model was used and thermal conduction effects where neglected. A fixed time step with 2nd order implicit scheme was imposed for both cold flow simulations. A time step of 1e^{-7}s was initially imposed and gradually increased every 10 timestep up to a final value of 2e^{-5}s to ensure the solutions stability and computational efficiency. Reactive flow simulations initiated after converged cold flow simulations used explicit time-stepping with a fixed value of 2e^{-9}s to ensure the numerical stability. Direct ignition was used for the detonation initiation by patching a small region of the flow with post detonation conditions as calculated by the NASA Chemical Equilibrium Application for the averaged local conditions [9]. Finite rate chemistry with Arrhenius reaction rates was employed to accurately resolve the combustion phenomena within the detonation engine. O'Conaire 9 species, 19 step reaction Hydrogen-oxygen mechanism was used to model the chemical reactions [10].

2.2. Computational domain and boundary conditions

The pulse detonation engine geometry investigated for this study was adapted from the experimental model developed by COMOTI (Romanian Research & Development Institute for Gas Turbines) [11]. The geometry includes a resonator mixer chamber composed of two oxidizer inlets and one fuel intake perpendicular to them in order to efficiently mix the fuel and oxidizer in a limited volume using fluidic resonances. The reactive mixture is discharged on a detonation ignition section (48 mm in length) downstream of the mixing chamber followed by a detonation tube of 500 mm with a diameter of 15.2 mm (Fig. 1-a).

The computational domain of the entire engine was built using Ansys Fluent Watertight. Poly-hexcore elements was utilized to discretize the computational domain due to their geometrical efficiency defining complex 3D volumes. Two mesh versions, with and without the outlet plenum, were created to effectively asses cold and reactive flow development within the current study to reduce the computational burden for the cases considered. Both meshes has the same PDE mesh structure depicted in Fig. 1 b and c while the one with plenum included a rectangular domain having a 500mm extension downstream of the engine, 195mm upstream and 300mm up, down, left and right form the engine centerline. This provides ample space for the detonation wave to exit and expand without significant boundary condition interaction.

The elements within the PDE were sized based on the theoretical detonation cell size of the reactive mixture. The cell size for pure Hydrogen-Air detonation at standard atmospheric conditions is about 2mm. As such, for the original mesh, we choose a target cell size of 600µm for the hexahedral cells. To minimize the amount of polyhedral cells in the mesh that present detrimental properties for detonation simulation, the minimal amount of peel layers was used and no boundary layer was implemented within the detonation tube. Boundary layer mesh is still present within the injection part of the engine to properly model the mixing of fuel and oxidizer in the vicinity of engine walls. This produces a PDE mesh of about 380k elements and a mesh of 1.1 million elements for PDE mesh including the discharge plenum. The plenum was configured to use 2mm cells, with the mesh expanding from the 300µm engine mesh to the largest plenum cell by doubling the cell size every 10 cells.

An automatic mesh refinement was configured for the detonative case to maximize resolution around the detonation front while limiting overall compute cost (see Fig 1-b). The mesh refinement trigger was set for any cells with a pressure above 15 Bar. This would get the cells subdivided according to Fluent's Adaptative Mesh Refinement (AMR) settings, up to two times. This means that a cell with an original size of 600µm can have a minimum size of 150µm, up to a maximum of 1.3M cells at a computational instant within the reactive simulations. This is only configured to occur within the thrust tube and the plenum but not at the injectors.

Boundary conditions were set to have one pressure inlet for hydrogen injection, two pressure inlets for oxygen injectors. Non-reflective pressure outlet boundary condition was used for the exhaust and plenum surfaces (Fig. 1 a). All the walls within the PDE are set to be adiabatic and no-slip. The hydrogen inlet was setup with 8.5 bar of pressure, while the oxygen inlets used 3.5 bar. All the gas is provided at a temperature of 300 K. The simulation pressure outlet is situated directly at the end of the trust tube and is setup with a pressure of 101325 Pa (1 atm) at 300 K.

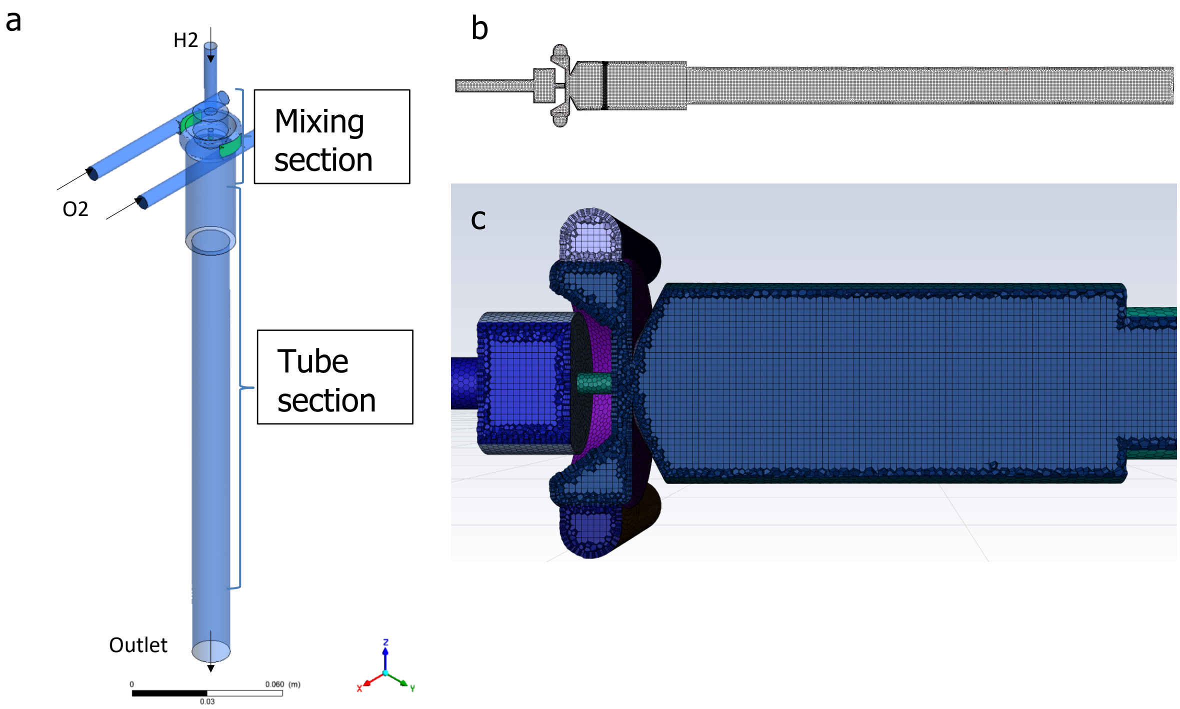

Fig. 1. a) Engine view and boundary conditions b) Computational Domain c) Close-up of the Mixing/Injection section (Mesh 4)

2.3. Mesh independence study

A through mesh independency study was conducted to make sure the results obtained in this study are free of variation from the computational cell size and computationally efficient as the reactive detonation simulations can generate a sizeable computational burden due to extremely low time steps and significant number of species continuity equations to be solved along with Navier-Stokes equations. The mesh independency study was conducted over the PDE geometry without an outlet plenum. In total 6 computational grids were studied to test over a wide range of cell sizes. Both cold flow and reactive flow conditions were studied for each case. The attributes of the meshes created for this work were summarized below. The reported grid sizes does not include instantaneous augmentation due to AMR, that refines each grid up to a quarter of the initial cell size. Due to the use of an explicit solver, the timestep was changed for the mesh independency study to ensure the numerical stability of the simulation. The underlined meshes were finally selected for further simulations as a result of grid convergence study detailed below.

- Mesh 1 – Coarsest mesh ~9k elements (cell size : 2mm)
- Mesh 2 – Coarse mesh ~40k elements (cell size : 1.2mm)
- Mesh 3 – Medium mesh ~100k elements (cell size : 900µm)
- <u>Mesh 4 – Fine mesh ~380k elements (cell size : 600µm)</u>
- Mesh 5 – Finer mesh ~700k elements (cell size : 450 µm)
- Mesh 6 – Finest mesh ~2.4M elements (cell size : 300µm)
- <u>Mesh 7 – Fine mesh with plenum ~1.1M elements (cell size : 600 µm)</u>

For the purposes of quantifying mesh convergence, the following values were recorded: species mass flow rates, injector P, T, M as well as the thrust tube P, T, M. Oxygen mass flow rate and equivalence ratios are selected to be the figures of merit for the grid convergence study. As depicted on Fig 2. the O2 mass flow rate converges with a very coarse mesh, while the H2 flow rate converges later in between the 380k and 700k element meshes. Analysis of the pressure field within the thrust tube present oscillations beginning with the 380k mesh. These oscillations are generated by the acoustic resonators presents within the injectors. As a result of the mesh independency study Mesh 4 with 380k element and Mesh 7 with 1.1 million elements (including the plenum) were selected to be used for the rest of the simulations in this study.

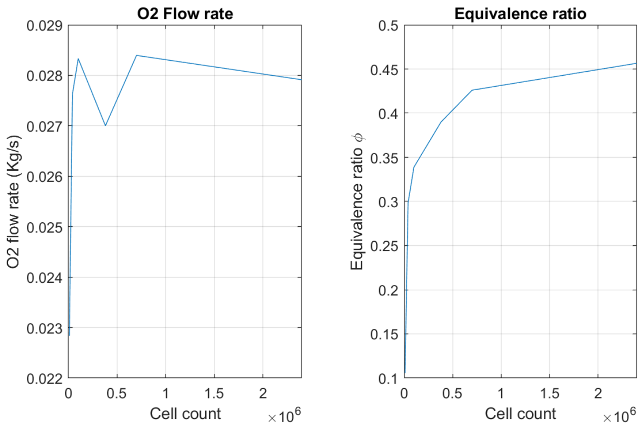

Fig 2. Variation of O_2 flow rate and equivalence ratio for various computational grids

2.4. Unsteady data acquisition and probe locations

Various flow properties were recorded at multiple points along various sections of the PDE in order to understand the evolution of the flow filed during the entire transient operation of PDE. These data include: mass flow rates for both oxygen injectors and the hydrogen injector depicted in (Fig 1-a) temperature, Mach number and pressure at 13 locations depicted in Fig 3, the pressure field along the centerline of one of the oxygen injectors, as well as the temperature, Mach number and pressure along the centerline of the tube for the reactive simulations. The purpose of the midline samplings is to track the propagation of the detonation wave along the tube, while the 13 probes were recorded for the purpose of doing a Short Time Fourier Transform (STFT) to produce spectrograms and study the periodic effects during the injection process. These probes are named using the following nomenclature: L1-L4 for the left injectors where L1 is the closes to the intake and L4 is the closest to the resonator end, similarly R1-R4 for the right injector. Mixer probes are named using the cardinal coordinates: N, E, S, W and C. N through W stand for North, West, and henceforth. C means Center and represent the probe at the middle.

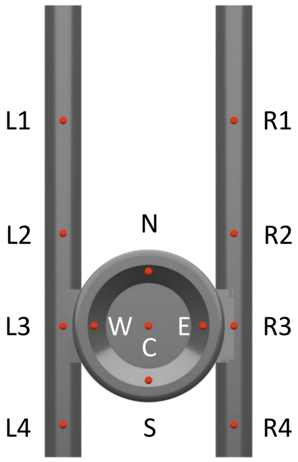

Fig 3. Probe locations along the injectors and mixer components

At the same time, the mass flow rate for each Oxygen injector and Hydrogen injector was recorded separately. The mass flow rate for the mixture exiting the tube was also acquired for both hydrogen and oxygen to ensure proper calculation of the reacting mixture at any point of the simulation. This is important as the cold flow simulation leaks fuel before detonation. The tube centerline was also probed at 7 locations to provide measurements for the detonation advancement down the detonation tube (Fig. 4).

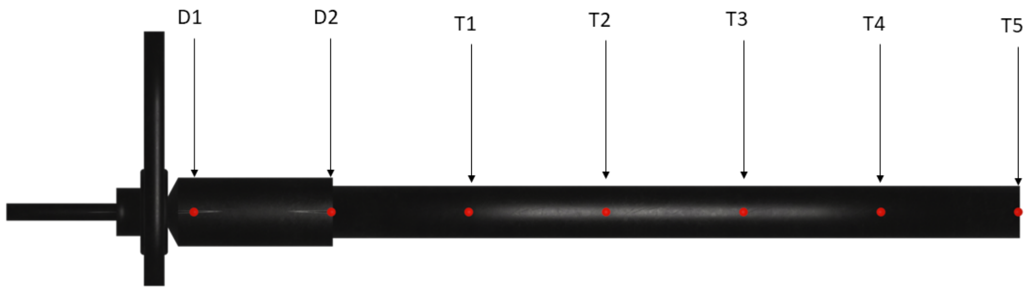

Fig 4. Probe locations along the ignition chamber and detonation tube

3. Results

3.1. Cold flow analysis

The hydrogen injector, presenting high pressure and a narrow inlet is chocked and as such isolating upstream from the rest of the flow. This is not true however for the two oxidizer injectors, as they are much lower pressure and present much wider effective flow area. This means that increasing H2 injection pressure also increases O2 mass flowrate by suction. This suction presents interesting dynamics that are beneficials for mixing . A periodic unsteadiness was created within the mixing zone that oscillates the incoming air streams consequently creating high vorticity with alternating motion of fluid which then enhances fuel-oxidizer mixing. Downstream of the mixing zone, perpendicular to the oxidizer stream, flow discharged to the ignition section through a tiny orifice at supersonic speed. Due to unsteadiness induced by the resonator, the supersonic jet shows an oscillatory motion upstream of the ignition zone which in turn further improves homogeneity of the reactants prior to the ignition location (Fig 5, Fig 6b, Fig 9). Following the initial transient of the simulations, the pressure level on the oxidizer ducts each side reaches a quasi-steady state with an oscillatory trend (Fig 6a).

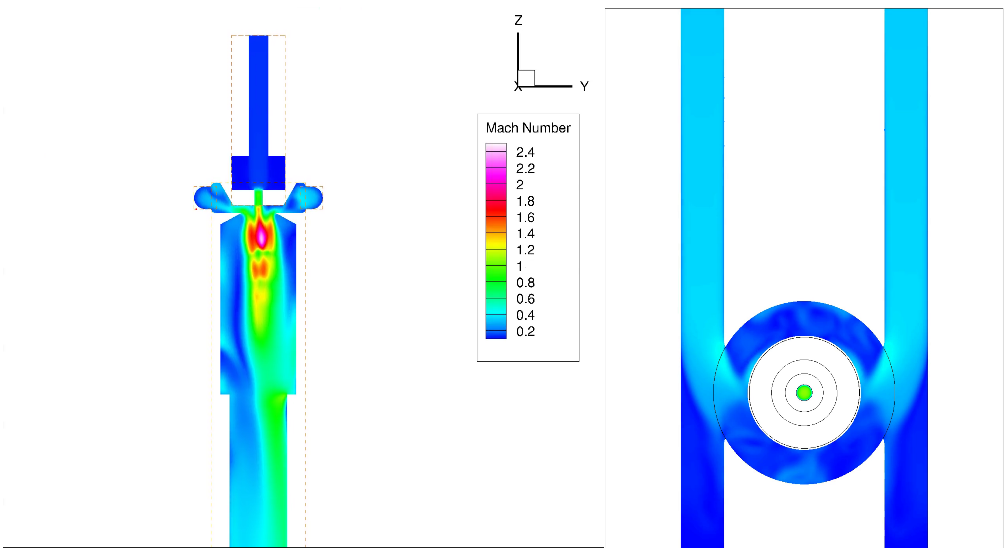

Fig 5. Mach number contours near the injector during the quasi-steady state feed

The unsteady behavior on the oxidizer lines is further analyzed using Short Time Fourier Transform (STFT) to investigate the frequency content of various flow quantities throughout the flow time (Fig 7 and Fig 8). The dominant frequencies on all quantities majorly clusters around 1kHz range which constitutes for an order of magnitude higher unsteadies beyond the operational range of PDE, which ensures mixing of the reactants is reached before the next ignition is initiated.

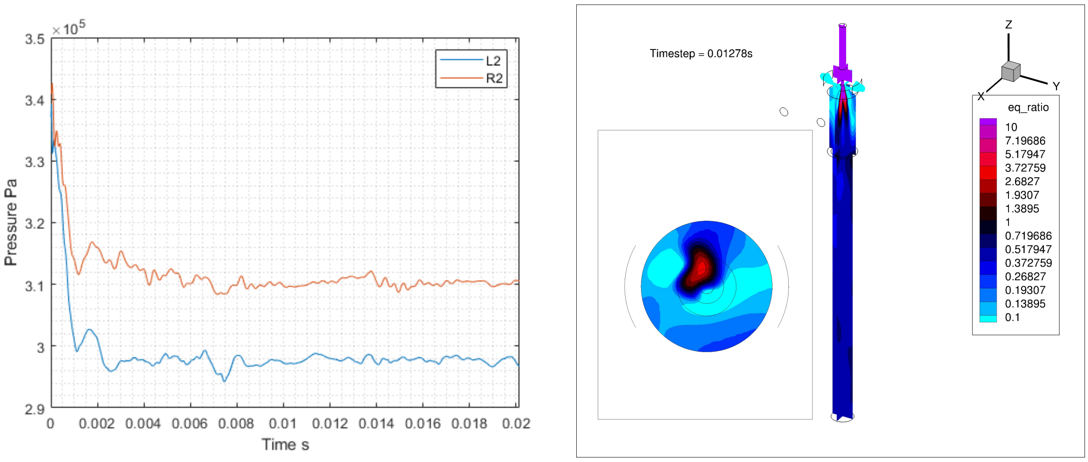

Fig 6. a) Pressure oscillations at L2 & R2 probes b) equivalence ratio during the injection

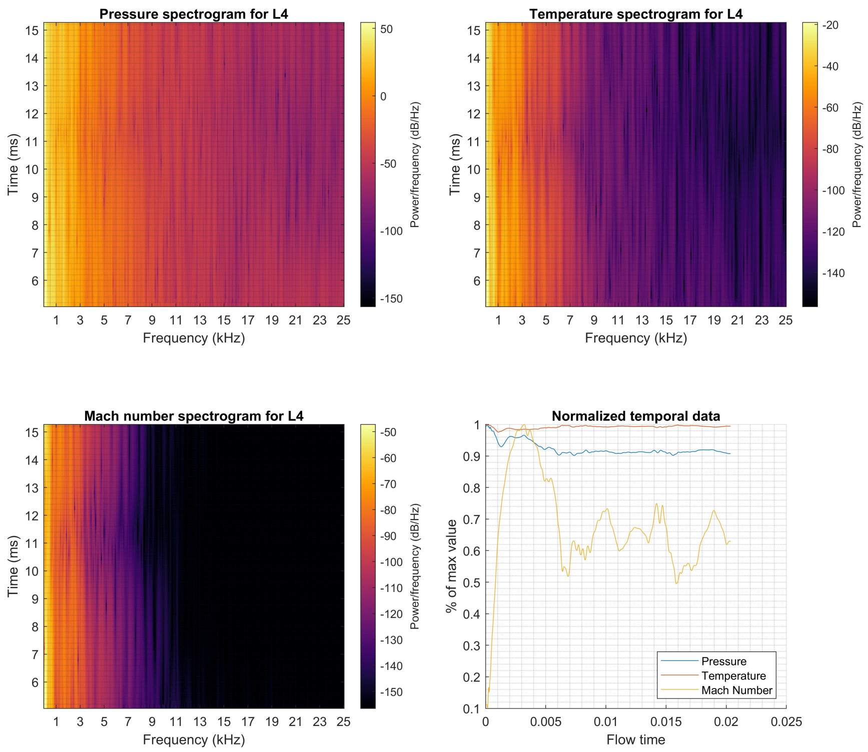

Fig 7. STFT spectrograms for P,T,M at L4 for the PDE geometry with plenum

The overall mass flow rate on the injectors and the resulting equivalence ratios at the ignition zone are provided in Fig 10. The mass flow traces clearly shows an oscillatory behavior around a mean value for the oxidizer stream once the initial transient is completed while the hydrogen streams show rather constant mass flow as expected from the chocked discharge. At the given operating conditions, the equivalence ratio, in turn, lands around a value slightly less than 0.4 and shows rather mild oscillations inherited from the oxygen lines. This shows a mixture quality ready for detonation at the ignition zone.

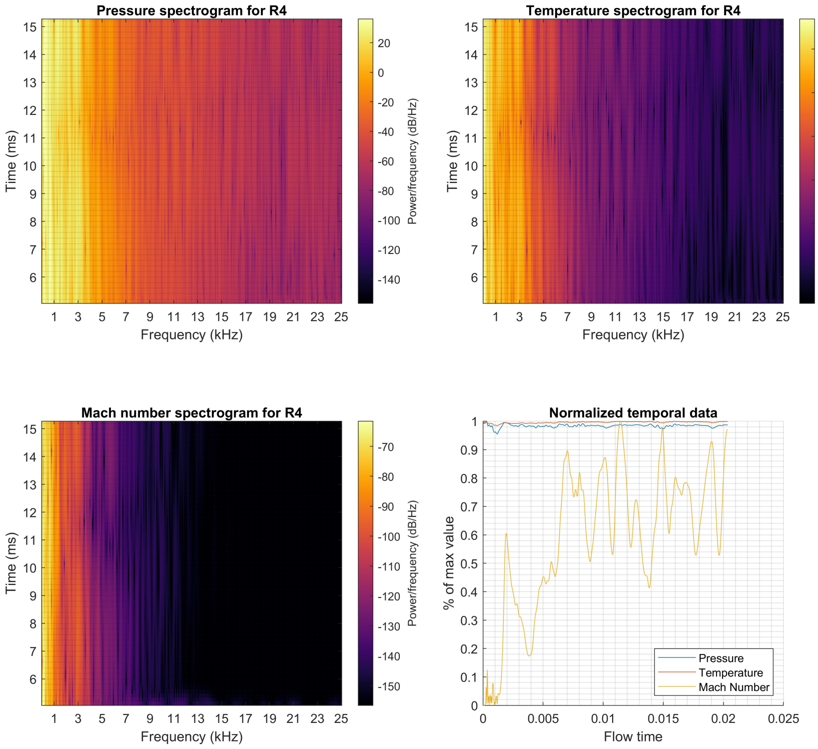

Fig 8. STFT spectrograms for P,T,M at R4 for the PDE geometry with plenum

The cold flow simulations were repeated to understand propulsive performance of the PDE using a computational domain including a discharge plenum (Mesh 7). Majority of the flow domain initially filled with nitrogen to imitate a prior purge cycle which cleans the duct from any residual high-temperature combustion products. For these simulations, the ignition zone was filled with a detonable mixture of hydrogen and oxygen within 1.9 ms flow time. Some residual nitrogen from the initialization is present in the tube and as such detonation at that time would result in different performance than expected. The cold flow was further advanced to make sure the residual nitrogen is discharged to the plenum. The injection reaches quasi-steady state at 2.5ms. The tube is filled with a homogeneous mixture at 3.3 ms and the residual nitrogen is almost fully expelled. This time extension causes a small fuel leakage to the plenum. Consequently, a performance abatement (I_{sp}) can be expected as fuel is lost and reaction outside the engine can be observed. The extra time given to the simulation that allows fuel leakage was mainly to investigate the unsteady injection over a longer period. The leaked fuel has been recorded to allow for more precise calculations. At the end of the simulation, the mixture quality present in the tube amounts to 58.73 mg of O_2 and 2.42 mg of H_2.

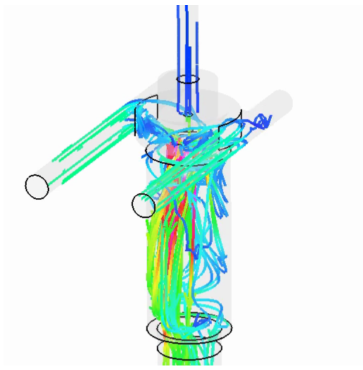

Fig 9. Streamlines of the cold flow

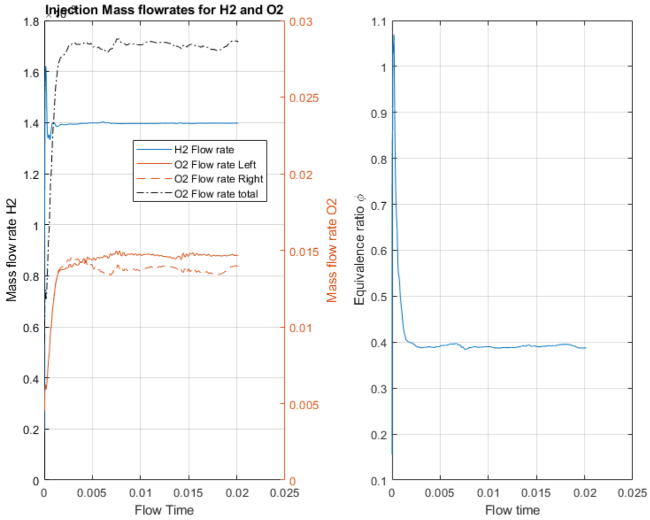

Fig 10. Left: injection mass flow rates Right: Injection equivalence ratio

3.2. Reactive flow analysis

The detonation was initiated at the end of the cold flow simulations with discharge plenum explained in the previous section. In effect, the cold flow served as initialization for the hot flow simulation. Direct Detonation Transition was used to for the simulation to mimic the spark ignition utilized in the experimental studies [12].The detonation was triggered by patching a thin layer (one cell thick, 600µm) of the flow with post-detonation conditions as computed by the NASA CEA software [9] using the C-J conditions which resulted in the following species concentrations summarized in the Table 1.

Table 1. Initial detonation patch conditions

Species	H	HO2	H2	H2O	H2O2	O	OH	O2	O3
Mass fraction	0.02%	0.06%	0.08%	28.34%	0.004%	1.91%	6.29%	63.30%	0,001%

These species were patched with a pressure of 21.1 bar and a temperature of 3163 K representing the C-J conditions at the location of the detonation plane with an equivalence ratio (ϕ) of 0.3. Due to way the injection is happening within the engine, a thin layer of stoichiometric mixture is present around the H2 jet. This more reactive region of the flow allows the detonation to progress faster during the initial instants of the detonation and generating a detonation wave with very pronounced 3D features (Fig 11).

The peak pressure recorded from the centerline probes (Fig 4) was 19 bar, with a peak temperature of 3400 K. However, the peaks encountered within the 3D detonation wave structure exhibits slightly higher level, at around 24 bar and 3500K, due to the curved detonation wave encountering its reflection and generating intense local hotspots. The simulations resulted in a wave speed of 2638.66 m/s which is quite a bit above the expected C-J conditions of 2032.8 m/s and is the evidence of an overdriven detonation wave. This behavior can be explained due to the geometry of the engine and the strong 3D features. Detonation results are in line with the expected C-J conditions for measured injection equivalence ratio while some local hotspots are observed due to the heterogenous mixing. Detonation front develops around the hydrogen injection jet, where the mixing between the oxygen and hydrogen jet locally generates stoichiometric conditions. This coupled with the instabilities of the injection produced very defined 3D features for the detonation wave (Fig 11).

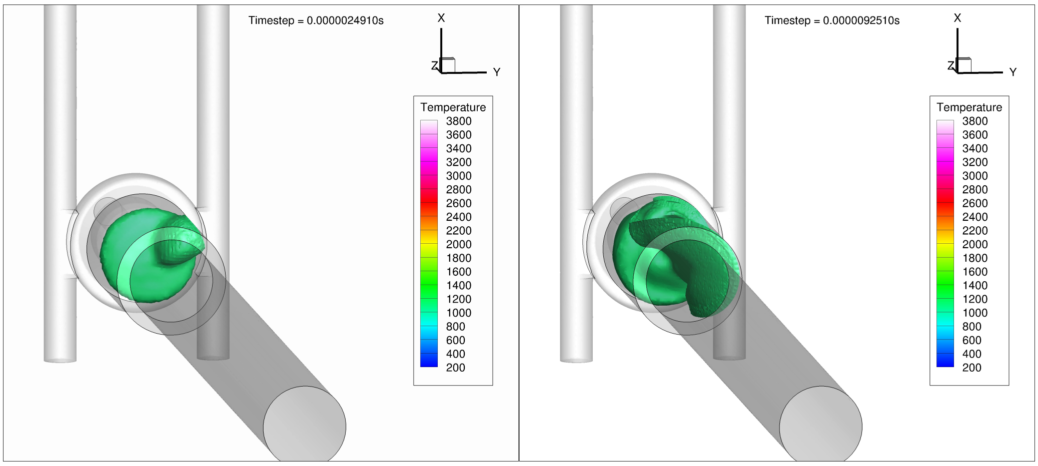

Fig 11. 13 bar Iso-surface colored in temperature, showing the detonation front 9.25 µs after detonation initiation.

Instantaneous thrust generated by the PDE is calculated throughout the computation's runtime. Fluent's integrated thrust calculation utility, integrating the pressure over the engine walls, and projecting it along the thrust axis was used to calculate the evolution of thrust (Fig 12-left). The thrust generated by the PDE shows an instantaneous peak value at around 200 N when the detonation wave discharged to the plenum and then gradually reduced towards lower values while the hot high-speed produces are expelled continuously. A valley on the thrust curve was reached around 40 N when the major combustion product flow is completed. The thrust production continues by the PDE thanks to the steady reactant flow by the injector system.

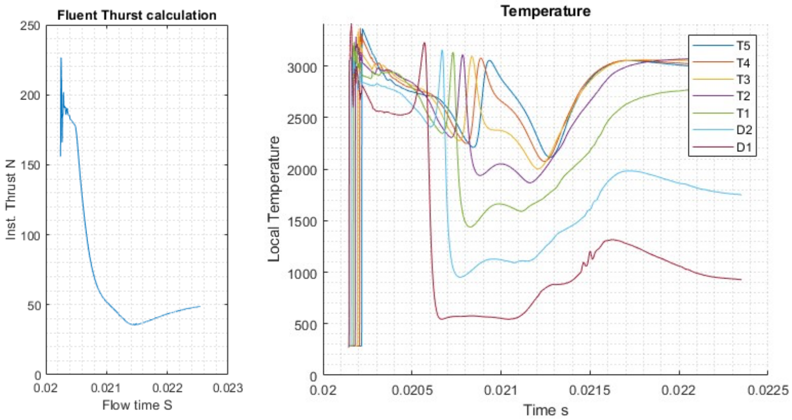

Fig 12. Left) Instantaneous thrust calculation, Right) Temperature field probed during the detonation

Using these calculations, the fuel specific total impulse generated by the engine during the simulations could be estimated around 0.0964 N.s by performing numerical integration of the instantaneous thrust obtained. The fuel and mixture specific I_{SP} calculations were performed using Eq 1 & 2.

$$I_{sp_{fuel}} = \frac{I}{g_0 * m_{H_2}} \tag{1}$$

$$I_{sp_{mixture}} = \frac{I}{g_0(m_{H_2} + m_{O_2})} \tag{2}$$

Using the mixture masses obtained earlier and with a g_0 value of 9.80665 m.s^{-1}, we obtain a fuel specific I_{sp} of 4061.5s and a mixture specific I_{sp} of 160.73s. The impulse continues for the entire rest of the simulation, for a total recorded impulse of 2.9644 ms. This gives us an average thrust of 32.5 N, calculated by taking the above total impulse and dividing it by the impulse time. These results are within expectation, both for impulse time and specific impulse [12]. No Negative impulse was recorded during the simulations and further compute time should be allocated to explore this behavior further.

A part of the fuel is leaked to the plenum during the injection cycle. This creates reactive flow out of the enclose thrust tube and generates no useful thrust. The reactive flow progresses further down the plenum that would otherwise happen with a fully inert compound. The flow in these parts is still very hot, at around 3000K. The pressure however drops quickly as the detonation decays to deflagrative combustion, slowly decreasing to near atmospheric conditions. Due to the way the simulation is setup, this can only happen during single pulse calculations. A further multi-pulse study might have a behavior similar to this leakage, but an a far more limited time frame due to injection timing constraints.

Although the pressure wave from the detonation diminishes rapidly, reaching 1.5 bars within 1.5 milliseconds, the tube temperature remains elevated at 3000K as the injection transitions to deflagrative combustion. It's worth mentioning that the temperature temporarily decreases to a minimum of 500K at the D1 probe during the initial phase of the blow down (Fig 12-right).

4. Conclusions

A series of three dimensional unsteady reactive flow simulations were performed over a realistic PDE design using acoustic resonator feed and mixer component using Ansys Fluent solver. Cold flow simulations showed a clear evidences of acoustic resonances within the oxidizer line and mixing zones. Oscillations of pressure, temperature and Mach number was observed in the injection part of the engine as well as in the ignition chamber. Spectral analysis of P, T and Mach numbers was performed to characterize the presence of acoustic resonance in the system. Coupling of the oxidizer and fuel injection was uncovered certain benefits, allowing a full injection cycle to be achieved in under 3.3ms. Detonation characteristics were investigated, using a direct detonation initiation. Results showed good agreement with theoretical Chapman-Jouguet detonation parameters, with increased detonation wave speed, indicative of an overdriven detonation due to hot spot occurring inhomogenously mixed zones in the PDE. Thrust and specific impulse calculation were performed using the mass flux integral at the PDE outlet. Computations show fuel specific impulse of 4061s with a mixture specific impulse of 160s achieved by the system. An average thrust delivered over 3ms PDE operation time was operated was calculated 32.5 N, with peak instantaneous thrust of 200 N. Additional future CFD studies using a different numerical approach to further deepen the understanding of recirculation zones, complex resonation and turbulent flow within the injector could allow the creation of more compact and more efficient pulse detonation engine with a limited injection cycle as reported in this work. Further work on prolonged operation of the PDE can uncover more insights about the longer duration cycles with periodic ignition by capturing the post-detonation blowdown within the plenum and purge cycle and thus conclude on the efficiency of the system at atmospheric and vacuum conditions.

5. Acknowledgement

The authors thank to the financial support of European Space Agency through contacts 4000131302/20/NL/MG which made this research possible.

References

[1] Kailasanath, K., Review of propulsion applications of detonation waves*,* AIAA journal, Vol. 38, pp. 1698–1708. (2000)

[2] Bussing, T. and Pappas, George, An introduction to pulse detonation engines 32nd Aerospace Sciences Meeting and Exhibit. p. 263. (1994)

[3] Morrison, Richard B., Adamson JR, Thomas C. and Weir JR, Alexander**.** Detonative and deflagrative combustion. ACS Publications, (1958)

[4] Roy, G., Frolov, S., Netzer, D., & Borisov, A. High-Speed Deflagration and Detonation. ELEX-KM Publishers (2001).

[5] Phillips, Bert R. / Pavli, Albert J. Resonance tube ignition of hydrogen-oxygen mixtures, 1971-05, No. TN D-6354 NASA, NASA (1971)

[6] Barr, L., "Pulse detonation engine flies into history," Press Release, Air Force Material Command, https://www.af.mil/News/Article-Display/Article/123534/pulsed-detonation-engine-flies-into-history/ (2008), Accessed 4 April 2024

[7] Roy G. D., Frolov S. M., Borisov, A. a., Netzer, D. W. Pulse detonation propulsion: challenges, current status, and future perspective, Progress in Energy and Combustion Science, Vol. 30, No. 6 p. 545-672 (2004)

[8] Coleman, M. L. "Overview of pulse detonation propulsion technology." (2001)

[9] Sanford Gordon and Bonnie J. McBride, NASA CEA run application https://cearun.grc.nasa.gov/ (2023), accessed 7 August 2023

[10] Ó Conaire, M., Curran, H. J., Simmie, J. M., Pitz, W. J., & Westbrook, C. K. A comprehensive modeling study of hydrogen oxidation. International journal of chemical kinetics, 36(11), 603-622. (2004)

[11] Cojocea, A. V., Cuciuc, T., Porumbel, I., Gall, M., Gherman, B., & Crunţeanu, D. E. Experimental Investigations of Hydrogen Fuelled Pulsed Detonation Combustor. In Turbo Expo: Power for Land, Sea, and Air (Vol. 86007, p. V03BT04A020). American Society of Mechanical Engineers (2022)

[12] Bussing, T., and George Pappas. "An introduction to pulse detonation engines." 32nd Aerospace Sciences Meeting and Exhibit. 1994.